Set Compliance Current Induced Resistive Memory Characteristics of W/Hf/HfOx/TiN Devices

S. Maji[1], S. Samanta[2], P. Das[1], S. Maikap[2], V.R. Dhanak[3], I.Z. Mitrovic[4], R. Mahapatra[1,a)]

[1]Department of Electronics and Communication Engineering, National Institute of Technology Durgapur, 713209, India

[2]Thin Film Nano Tech. Lab., Department of Electronic Engineering, Chang Gung University, 259 Wen-Hwa 1st Rd., Kwei-Shan, Tao-Yuan, 333, Taiwan

[3]Dept. of Physics and Stephenson Institute for Renewable Energy, University of Liverpool, Liverpool L69 7ZF, UK

[4]Department of Electrical Engineering and Electronics, University of Liverpool, Liverpool L69 3GJ, UK

[a)] Electronic mail: rajat.mahapatra@ece.nitdgp.ac.in

In this paper, we have investigated the effect of current compliance during set process on resistive memory characteristics and switching mechanism of W/Hf/HfO_x/TiN devices. The presence of Hf thin cap layer enables the stable and uniform bipolar resistive switching behaviour. Compliance current can modify the barrier height at oxide-electrode interface by increasing or reducing the oxygen vacancies and induce different switching mechanisms. Low compliance current (50μA) based switching confirms Schottky conduction mechanism due to the interfacial effects while high compliance current (500μA) involves the ohmic conduction mechanism, signifying the formation of conductive filament. No significant dispersion of reset current and reset voltage has been found for each set compliance current varying from 50 μA to 500 μA, indicating uniform performance of the devices. The devices also exhibited read endurance up to 2000 cycles.

I. INTRODUCTION

Recently resistive random access memory (RRAM) has emerged as a potential replacement of flash memory in next-generation non-volatile memory (NVM) applications due to its simple metal-insulator-metal (MIM) structure, low operating power, high speed, and three dimensional stackability.[1-5]Among different oxides, HfO_2 has a strong potential for resistive memory applications due to its compatibility with Si-based complementary metal-oxide-semiconductor (CMOS) technology, high scalability, and low-energy dissipation.[6,7] Despite its promising future, great challenges including the varied resistance distribution as well as the non-uniformity of the set and reset voltages still remain to be undertaken. The metal top capping layers (Hf, Ti) are regarded to significantly improve the resistive switching effect, enabling the redox reactions at the interface between the top electrode (TE) and oxide layer through the formation of an ionic reservoir.[8,9] Although the detailed switching mechanism of RRAM remains ambiguous, it is widely recognized that the migration of oxygen vacancies under an applied electrical field are accountable for the switching behaviour.[10] The field driven local accumulation or depletion of oxygen vacancies in switching layer defines the two resistance states namely low resistance state (LRS) and high resistance state (HRS).In order to improve the stability of the resistive switching phenomenon, a critical amount of oxygen vacancies needs to be produced inside the oxide film.

The memory characteristics and mechanism can be controlled by tuning the voltage range and/or current compliance used during forming/set operation. Bishop *et* al.[11] have studied the influence of set current on reset characteristics of TaO_x based resistive switching devices. Su *et* al.[12] have reported that the conduction mechanism in low resistance state of set cycle changes from hopping to surface scattering and finally to ohmic conduction in $TiN/HfO_x/TiN$ resistive switching devices. However, they have not reported the influence of set current on the reset characteristics. Raghavan *et* al.[13] presented the presence of two

different independent switching mechanisms in metal-insulator-semiconductor (MIS) RRAM device which depend on the compliance current for forming/set transition. Low compliance current based switching involves oxygen vacancy mediation while high compliance current switching includes formation and rupture of conductive metallic filaments. It has been proposed that the reduction or increase in oxygen vacancies may alter the Schottky barrier height at the oxide-electrode interface and could thereby control the device resistance.[14,15]

In this article, the influence of set compliance current on resistive switching characteristics and its mechanism of W/Hf/HfOx/TiN devices have been reported. The W and TiN have been used as both are CMOS compatible. The effect of reactive capping layer of Hf on memory performance between both W/HfO_x/TiN and W/Hf/HfO_x/TiN has been investigated. Also, the effect of different compliance currents on resistive switching characteristics of W/Hf/HfO_x/TiN device has been explored. Finally, we report on the switching mechanism in both set and reset cycle depending on the compliance current.

II. EXPERIMENTAL

The resistive switching devices using Hf/HfO_x as switching oxide , titanium nitride (TiN) as a bottom electrode (BE), and tungsten (W) as a top electrode (TE) have been fabricated in via-hole structure. A TiN layer BE of about 200 nm was deposited on 8 inch SiO_2(200 nm)/Si wafer by RF sputter system. Next, a layer SiO_2 of 150 nm was deposited on TiN BE. Different via sizes from 0.4 to 4 μm and BE contacts were patterned by lithography and dry etching processes followed by another lithography step to pattern the devices for HfO_x deposition. In this stage, single layer of HfO_x and bi-layer of Hf/HfO_x were deposited to fabricate two set of devices. The single HfO_x layer (~7.5nm) was deposited by reactive RF sputtering of Hf target with Ar and O_2 gas with flow rate of 20 sccm and 5 sccm, respectively. The Hf layer (~3nm) was deposited on HfO_x layer by sputtering of Hf in Ar environment to fabricate bi-layer of Hf/HfO_x. Then, a W layer of nominal 100 nm was deposited by RF

sputtering of W target in Ar gas. Finally, the lift-off process was carried out to fabricate $W/HfO_x/TiN/SiO_2/Si$ and $W/Hf/HfO_x/TiN/SiO_2/Si$ pristine resistive switching devices. Fig. 1 shows the high-resolution transmission electron microscope (HRTEM) micrograph of the deposited HfO_x switching material. The thickness of HfO_x was determined to be ~7.5 nm with some local crystalline formation.

The chemical composition of HfO_x and Hf/HfO_x layers were characterized by x-ray photoelectron spectroscopy (XPS) analyses. XPS measurements were performed in an ultra-high vacuum chamber consisting of a Al K_αX-ray source, a PSP Vacuum Technology hemispherical electron energy analyser equipped with a 5-channeltron detector, and an Ar ion sputter gun. The spectrometer was calibrated using a sputtered silver foil. The spectra were taken in the normal emission geometry at a fixed pass energy of 20 eV, corresponding to a resolution of about 0.2 eV. The analysis followed a Shirley type background correction before line-shape fitting with Voigt functions. The Casa XPS software, version 2.3.17 PR1.1, was used for all data analysis. All electrical characteristics of the resistive switching devices were measured using an Agilent B1500A semiconductor parameter analyzer with biasing at the TE and grounding at the BE.

III. RESULTS AND DISCUSSION

Fig. 2 (a) shows the typical bipolar resistive switching behaviour of $W/HfO_x/TiN$ and $W/Hf/HfO_x/TiN$ resistive memory devices of sizes 0.4µm x 0.4µm with set compliance current (CC) of 500µA. The arrow in the figure signifies the voltage sweep direction. The devices switch from high resistance state to low resistance state at positive set voltage (V_{Set}) and the devices switch back from LRS to HRS at negative reset voltages (V_{Reset}). Prior to switching cycles, the electroforming was carried by applying a positive voltage in pristine devices with a current compliance of 50 µA. The forming voltages were found to be of 3.0 V and 3.3 V for $W/HfO_x/TiN$ and $W/Hf/HfO_x/TiN$ resistive memory devices, respectively. Fig.

2(b) shows distribution of reset voltages of W/HfO_x/TiN and W/Hf/HfO_x/TiN RRAM devices with current compliance of 500μA. The measure of coefficient of variance (σ/μ) for reset voltage of W/HfOx/TiN and W/Hf/HfOx/TiN structure devices are 3.15% and 2.61%, respectively. The resistive memory devices with Hf capping layer shows the uniform and lower reset voltages. Here, the Hf cap layer acts as an oxygen buffer layer that allows to obtain O-deficient non-stoichiometric HfO_x and to form a conducting path, switched on/off through V_O migration under electric field. In the reset cycle, more O^{2-} ions are available in Hf capping layers to break the conducting path which attributes to the lower and uniform reset voltages. The more uniform distribution of reset current has been observed in W/Hf/HfOx/TiN memory devices as shown in Fig. 2(c). The σ/μ values for reset current are found to be 3.2% and 1.62% for W/HfOx/TiN and W/Hf/HfOx/TiN devices, respectively. When the applied negative bias reaches reset voltages, the oxygen ions are driven down from Hf cap layer to combine with the oxygen vacancies in HfO_x layer and the devices are reset to high resistance state. The distribution of high resistance state and low resistance state measured at read voltage of -0.2V is presented in Fig. 2(d). The fluctuation of LRS was tighter than that of HRS, and the resistance ratio of HRS/LRS is higher for the resistive switching devices with Hf cap layer. This is attributed to the stronger conducting path in presence of Hf thin cap layer resulting in the lower values of resistances in LRS, enabling control of the O-deficiency level in the HfO_x as confirmed by the following XPS data.

Fig. 3 (a) and (b) show X-ray photoelectron spectra of Hf 4f core level (CL) from HfO_x and Hf/HfO_x layers, respectively. In the case of single layer HfO_x sample, the Hf 4f core level (CL) has been fitted with two spin orbit doublets attributed to the Hf^{4+} from stoichiometric HfO_2 and Hf^{x+} from non-stoichiometric oxide ($HfO_{x<2}$) as shown Fig 3 (a). The spin orbit splitting of the stoichiometric oxide is 1.63 eV with Hf 4f doublet intensity ratio (Hf $4f_{7/2}$: Hf $4f_{5/2}$) of 0.75. The peak of Hf $4f_{7/2}$ related to non-stoichiometric HfO_x has

been observed at 16.28 eV which is close to the reported values.[16-18] In comparison, the Hf 4f core level line-shape from Hf/HfO_x sample has been fitted with three different peaks attributed to Hf^{4+}, a sub-oxide Hf^{x+} and metallic Hf^0 as shown in Fig. 3 (b). The peaks related to the non-stoichiometric Hf^{x+} and metallic Hf^0 has been observed at binding energies ($4f_{7/2}$ position) of 16.13 eV and 13.80 eV, respectively, in agreement with reported values.[18] The values of binding energy of different peaks are shown in Table 1. A small shift of the Hf 4f core levels (CL) to the lower binding energy is observed for the bilayer sample, showing that the oxide is less stoichiometric in the bilayer sample. The percentage contributions of all peaks for different samples are shown in Table 2. The metallic Hf contribution is as less as 0.005% whereas HfO_x <2 percentage has changed significantly from 47.60% (HfO_x layer) to 64.82 (Hf/HfO_x layers). The XPS data strongly support the existence of more oxygen vacancies in bilayer (Hf/HfO_x) sample as compared to single layer (HfO_x) sample.

Table 1: Peak position of Hf^{4+}, a sub-oxide Hf^{x+} and metallic Hf^0

Sample	**Hf $4f_{7/2}HfO_{x<2}$**	**Hf $4f_{5/2}HfO_{x<2}$**	**Hf 4f $_{7/2}$ HfO_2**	**Hf 4f $_{5/2}$ HfO_2**	**Hf 4f $_{7/2}$ metallic**	**Hf 4f $_{5/2}$ metallic**
HfO_x	16.28 eV	17.94 eV	17.51 eV	19.14 eV	NA	NA
Hf/HfO_x	16.13 eV	17.79 eV	17.35 eV	18.98 eV	13.80 eV	15.51 eV

Table 2: Percentage of area contributed for different peaks

Sample	**Hf $4f_{7/2}HfO_{x<2}$**	**Hf $4f_{5/2}HfO_{x<2}$**	**Hf 4f $_{7/2}$ HfO_2**
HfO_x	47.60 %	52.40 %	0 %
Hf/HfO_x	64.82 %	34.63 %	0.005 %

Fig. 4(a) shows the current versus voltage (I–V) characteristics of the W/Hf/HfO_x/TiN device under different set compliance currents of 50 µA, 100 µA, 200 µA, and 500 µA. Even though the compliance current varies, polarizations of the resistive switching are similar with positive biasing in the set process and negative biasing in the reset process. Gradual transition during reset process is observed when compliance current is rather small (< 200 µA). However, the comparatively sharp transition is observed for the compliance current of 500 µA during set and reset processes. Fig. 4(b) shows the distribution of reset currents as a function of set compliance current. The device shows the uniform reset current for each individual CC. The reset current is approximately equal to set compliance current in W/Hf/HfO_x/TiN device signifying the reduction of compliance failure, while Gao et al.[19] have reported the compliance failure in W/HfO_2/Pt devices. It is also observed that the reset current increases and LRS resistance measured at read voltage of -0.2V decreases with compliance current as shown in Fig. 4(c). A higher set current compliance allows formation of stronger conductive path within the oxide which attributes to a lower resistance in LRS [20, 21] Fig. 4(d) shows the distribution of reset voltages as a function of set compliance current. The dispersion of reset voltages for individual set CC is not significant confirming the uniform results from device-to-device measurements. However, the reset voltages increase from ~ -0.75V to ~ -2.5V with increase in set current compliance from 50µA to 500µA. As a result, for higher set CC the device in LRS with stronger conducting path desires a higher reset voltage to retune the device back to HRS.

To investigate the current conduction mechanisms in W/Hf/HfO_x/TiN device, the I-V data were fitted in both set and reset regions. The Schottky emission was found to fit well at lower set CC of 50µA in both HRS and LRS as shown Fig. **5**. The barrier height was extracted from the following equation

$$J = A * T^2 \exp[-\frac{q\left(\emptyset_B - \sqrt{qE/4\pi\epsilon_0\varepsilon_r}\right)}{k_B T}]$$

where $A^*$is the effective Richardson constant, T is the absolute temperature, J is the current density, E is the electric field, $\emptyset_B$ is the effective Schottky barrier height, q is the electronic charge, ε_0 is the permittivity of free space, ε_r is the dynamic dielectric constant, k_B is Boltzmann's constant. The barrier height is extracted to be ~ 0.19eV in LRS for both set and reset regions while the barrier heights are 0.23 eV and 0.26 eV for set and reset regions in HRS, respectively. Fig. 6 shows the fittings of Schottky and ohmic conduction for W/Hf/HfO_x/TiN switching device at higher set CC of 500µA. The ohmic conduction dominates in LRS for both set and reset regions while the Schottky emission dominates in HRS with barrier height of 0.24 eV. The values of barrier height are also comparable with previously reported value (~ 0.29 eV) extracted from the Schottky emission.[22]

To highlight on interfacial and filamentary resistive switching, the resistance at LRS with different electrode sizes for current compliance currents of 50µA and 500µA was measured at -0.2V, as shown in Fig 7. The resistance at LRS for 50µA decreases as electrode sizes increase, indicating that the current is interfacial resistive switching throughout the device and the switching occurs on the entire thin film. Moreover, the polarity-dependent migration via oxygen vacancies induces oxygen-deficient/oxygen-rich region modulation, resulting in different resistivities. However, the resistance at the LRS for 500 µA was found to be independent of the device sizes resulting from the formation of localized conducting filaments [23, 24]. Fig 8 shows the reset current variation with electrode sizes for current compliance currents of 50µA and 500µA. The increase of reset current with electrode sizes for 50µA CC is second clear evidence of interfacial switching [24]. The slight variation of

the reset current with electrode sizes has been observed for 500μA CC. This can be attributed to the leakage current through the residual filaments or defects.

On the basis of the aforesaid analysis, the resistive switching mechanism of W/Hf/HfO_x/TiN device here can be explained in views of the development of oxygen vacancy conducting path controlled by compliance current, schematically shown in Fig 9. This is a critical parameter which tunes the amount of oxygen vacancies in the conducting path in the oxide layer during the resistive memory operation to attain stable switching.[25] There are two views on switching mechanism. Some suggest oxygen-vacancy mediated switching,[26-28] others suggest nucleation and rupture of metallic filaments to be the possible mechanism.[29,30] When the current compliance is set at the lowest 50μA, only a few oxygen vacancies are created [Fig. 9 (b)]. At lower compliance current of 50μA, it has been observed that the Schottky barrier is responsible for bipolar resistive switching of W/Hf/HfO_x/TiNdevice in both HRS and LRS. The lower barrier height is obtained in LRS while the higher barrier height is observed in HRS. The Schottky barrier is modulated when the when the oxygen vacancy are attracted to or repealed from the metal contact through the application of an electric field. This result indicates that lower compliance current switching is governed through interfacial conduction mechanism by Schottky barrier modulation between the top electrode and dielectric layer. In contrast, at higher current compliance of 500μA, the ohmic conduction in LRS is responsible for the formation of conductive filaments. It can be deduced that by increasing set current compliance, the Hf/HfO_x interface oxidation is boosted so that the metallic Hf gets oxidized and, as a result the oxygen vacancy concentration in HfO_x increases to form metallic conductive filament [Fig 9(c)]. During reset cycles, the oxygen ions are driven down from Hf cap layer to combine with the oxygen vacancies in HfO_x layer and the filaments are ruptured to form a Schottky barrier in HRS.

As cycle endurance is one of the highest urgencies of RRAM, especially for storage memory applications, pulse endurance characteristic of W/Hf/HfO_x/TiN resistive memory device was carried out at voltage -0.2V with 500µs pulse as shown in Fig. 10. It can be noticed that the resistance window remains stable up to 2000 cycles without observing any degradation. The average resistance ratio is found to be ~ 10.0.

IV. CONCLUSION

The resistive memory characteristics and switching mechanism of W/Hf/HfO_x/TiN device has thoroughly been investigated with different set current compliance. The presence of Hf thin cap layer enables the control of the O-deficiency level in the HfO_x layer which shows the stable and uniform bipolar resistive switching behaviour. No significant dispersion of reset current and reset voltage has been observed for each set compliance current varying from 50 µA to 500 µA. Analysis of conduction mechanisms of HRS and LRS of W/Hf/HfOx/TiN devices at 50 µA CC confirms that bipolar resistive switching both in HRS and LRS is dominated through interfacial effects by Schottky emission. At higher CC of 500 µA CC, the HRS is governed by Schottky emission and LRS by ohmic conduction due to formation of localized conducting filaments. Thus, it has been observed that set compliance current can modulate the barrier height at oxide-electrode interface by reducing or increasing oxygen vacancies and enable decoding of the different switching mechanisms in RRAM.

[1]R. Waser and M.Aono,Nat. Mater. 6 ,833 (2007)

[2]S. Kumar, C. E. Graves, J. P. Strachan, E. M. Grafals, A. L. D. Kilcoyne, T. Tyliszczak, J. N. Weker, Y. Nishi and R. S. Williams, Adv. Mater. 28, 2772 (2016)

[3] P. K. Sarkar, M. Prajapat, A. Barman, S. Bhattacharjee, and A. Roy, (2016), J. Mater. Sci. 51, 4411 (2016)

[4]Y. B. Zhu, K. Zheng, X. Wu and L. K. Ang, Sci. Rep. 7, 43664 (2017)

[5]S. Chakrabarti, S. Ginnaram, S. Jana, Z.Y.Wu, K. Singh, A. Roy, P. Kumar, S. Maikap, J.T.Qiu, H.M.Cheng, L.N.Tsai, Y. L. Chang, R. Mahapatra and J.R. Yang, Sci. Rep. 7, 4735 (2017)

[6]W. He, H. Sun, Y. Zhou, K. Lu, K. Xue and X. Miao, Sci. Rep. 7, 10070 (2017)

[7]Y.S.Chen, H.Y. Lee, P.S. Chen, T.Y. Wu, C.C. Wang, P.J.Tzeng, F. Chen, M.J Tsai, and C. Lien, IEEE Electron.Device.Lett. 31, 1473(2010)

[8] H. Y. Lee, P. S. Chen, T. Y. Wu, Y. S. Chen, C. C. Wang, P. J. Tzeng, C. H. Lin, F. Chen, C.H.Lien and M.J. Tsai, Tech. Dig. - Int. Electron Devices Meet. 297(2008)

[9]H. Y. Lee, P.S. Chen, T.Y.Wu, Y. S. Chen, F. Chen, C.C.Wang, P.J.Tzeng, C. H. Lin, M.J. Tsai and C. Lien, IEEE Electron Device. Lett. 30, 703 (2009)

[10]D. Ielmini, Semicond. Sci. Technol. 31, 063002 (2016)

[11]S. M. Bishop, H. Bakhru, J. O. Capulong and N. C. Cady,Appl. Phys. Lett. 100, 142111 (2012)

[12]Y.T. Su, K.C. Chang, T.C.Chang, T.M.Tsai, R. Zhang, J. C. Lou, J.H.Chen, T.F.Young, K.H.Chen, B.H.Tseng, C.C.Shih, Y.L.Yang, M.C.Chen, T.J.Chu, C.H.Pan, Y.E.Syu and S. M. Sze,Appl. Phys. Lett.103, 163502(2013)

[13]N. Raghavan, K. L. Pey , W. Liu , X. Wu, X. Li and M. Bosman, Microelectron. Eng.88, 1124 (2011)

[14]A. Sawa, Mater. Today,11, 28 (2008)

[15]J.J.Yang, M. D. Pickett, X. Li, D. A. A. Ohlberg, D. R. Stewart, and R. S. Williams, Nat. Nanotechnol. 3, 429 (2008)

[16]R.Zazpe, M Ungureanu , F Golmar , P Stoliar, R Llopis , F Casanova , D.F. Pickup ,C Rogero and L. E. Hueso , J. Mater.Chem. C, 2, 3204 (2014)

[17]M. Copel, R. P. Pezzi, D. Neumayer, and P. Jamison, Appl.Phys. Lett.,88, 072914 (2006)

[18]S. U. Sharath, T. Bertaud, J. Kurian, E. Hildebrandt, C. Walczyk, P. Calka, P. Zaumseil, M. Sowinska, D. Walczyk, A. Gloskovskii, T. Schroeder and L. Alff, Appl. Phys. Lett. 104, 063502 (2014)

[19] B. Gao, W. Y. Chang, B. Sun, H. W. Zhang, L. F. Liu, X. Y. Liu, R. Q. Han, T. B. Wu and J. F. Kang,International Symposium on VLSI Technology, System and Application, 144(2010)

[20]C. Rohde, B. J. Choi, D. S. Jeong, S. Choi, J.S. Zhao and C. S. Hwang, Appl. Phys. Lett.86, 262907 (2005)

[21]S. Roy , A. Roy, R. Panja, S. Samanta, S. Chakrabarti , P.L. Yu, S. Maikap, H.M.Cheng , L.N. Tsa and J.T. Qiu, J. Alloy Compd ,726, 30 (2017)

[22]X. Chen, W. Hu, Y. Li, S. Wu and D.Bao,Appl. Phys. Lett. 108, 053504 (2016)

[23]G. Sassine, S. L. Barbera, N. Najjari, M. Minvielle, C. Dubourdieu, and F. Alibart, J. Vac. Sci. Technol. B. 34, 012202 (2016)

[24]R. Huang, X. Yan, S. Ye, R Kashtiban, R. Beanland, K.A. Morgan, M. D. B. Charlton and C. H. (Kees) de Groot, Nano. Scale. Res. Lett.12, 384 (2017)

[25]M. Sowinska, T. Bertaud, D. Walczyk, S. Thiess, P. Calka, L. Alff, C. Walczyk and T. Schroeder,J.Appl.Phys.115, 204509 (2014)

[26]S. A. Mojarad, J. P. Goss, K. S. K. Kwa, P. K. Petrov, B. Zou, N. Alford and A. O'Neill, J. Appl. Phys. 112, 124516 (2012)

[27]G. Bersuker, D.C. Gilmer, D. Veksler, J. Yum, H. Park, S. Lian, L. Vandelli, A.Padovani, L. Larcher, K. McKenna, A. Shluger, V. Iglesias, M. Porti, M. Nafria, W.Taylor, P.D. Kirsch and R. Jammy,IEEE IEDM Technical Digest,456 (2010)

[28]C. Vallée, P. Gonon, C. Jorel, F.El. Kamel, M. Mougenot and V. Jousseaume, Microelectron. Eng. 86, 1774 (2009)

[29]D.H. Kwon, K.M. Kim, J.H. Jang, J.M. Jeon, M.H. Lee, G.H. Kim, X.S. Li, G.S. Park, B.Lee, S. Han, M. Kim and C.S. Hwang, Nat .Nanotechnol.5, 148 (2010)

[30]X. Li, W.H. Liu, N. Raghavan, M. Bosman and K.L. Pey,Appl. Phys. Lett.97, 202904 (2010)

Fig Captions:

Fig. 1 High-resolution transmission electron microscope (HRTEM) image of the deposited HfO_x switching material. The thickness of HfO_x was found to be ~7.5 ± 0.5nm.

Fig. 2(a) Bipolar switching behaviour of W/HfO_x/TiN and W/Hf/HfO_x/TiN RRAM devices. Cumulative probability plots of: (b) reset voltages, (c) reset currents, and (d) high resistance and low resistance measured at voltage of -0.2V.

Fig. 3 X-ray photoelectron spectra of Hf 4f core level for:(a) HfO_x and (b) Hf/HfO_x layers.

Fig. 4(a) Bipolar switching behaviour of the W/Hf/HfO_x/TiN device under various set compliance currents of 50 µA, 100 µA, 200 µA, and 500 µA. (b) Cumulative probability of reset currents as a function of set compliance current. (c) Variation of reset current and LRS resistance measured at measured voltage of -0.2V as a function of compliance current. (d) Cumulative probability of reset voltages as a function of set compliance current.

Fig. 5 Schottky emission plots for W/Hf/HfO_x/TiN device at set compliance current of 50µA: (a) High Resistance State of set cycle, (b) Low Resistance State of set cycle, (c) High Resistance State of reset cycle, (b) Low Resistance State of reset cycle.

Fig. 6 Current conduction mechanisms (Schottky and ohmic) fitting of I-V curves for W/Hf/HfO_x/TiN device at set CC of 500µA: (a) High Resistance State of set cycle, (b) Low Resistance State of set cycle, (c) High Resistance State of reset cycle, (b) Low Resistance State of reset cycle.

Fig. 7 Variation of resistance at low resistance state with different electrode sizes for current compliance currents of 50µA and 500µA measured at -0.2V.

Fig. 8 The reset current variation with electrode sizes for current compliance currents of 50µA and 500µA.

Fig. 9 Schematic diagram of the resistive switching mechanism of W/Hf/HfO_x/TiN device in views of the development of oxygen vacancy conducting path controlled by compliance current.

Fig. 10 Cycling endurance of W/Hf/HfO_x/TiN resistive memory device at measured voltage of -0.2V with 500μs pulse.

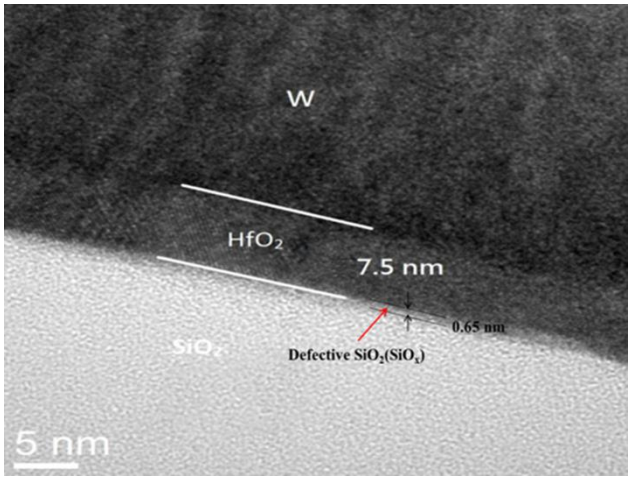

Fig. 1

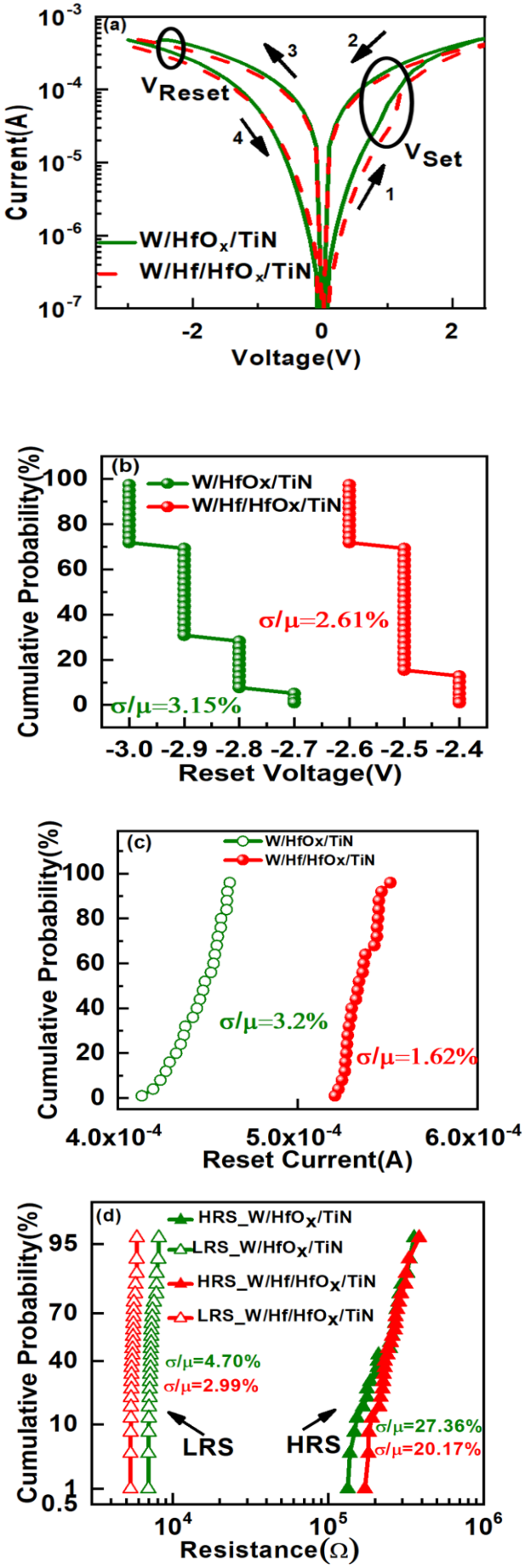
(a)
Current(A)
Voltage(V)
V_Reset
V_Set
1
2
3
4
W/HfO_x/TiN
W/Hf/HfO_x/TiN
(b)
Cumulative Probability(%)
Reset Voltage(V)
W/HfOx/TiN
W/Hf/HfOx/TiN
σ/μ=2.61%
σ/μ=3.15%
(c)
Cumulative Probability(%)
Reset Current(A)
W/HfOx/TiN
W/Hf/HfOx/TiN
σ/μ=3.2%
σ/μ=1.62%
(d)
Cumulative Probability(%)
Resistance(Ω)
HRS_W/HfO_x/TiN
LRS_W/HfO_x/TiN
HRS_W/Hf/HfO_x/TiN
LRS_W/Hf/HfO_x/TiN
σ/μ=4.70%
σ/μ=2.99%
σ/μ=27.36%
σ/μ=20.17%
LRS
HRS

Fig. 2

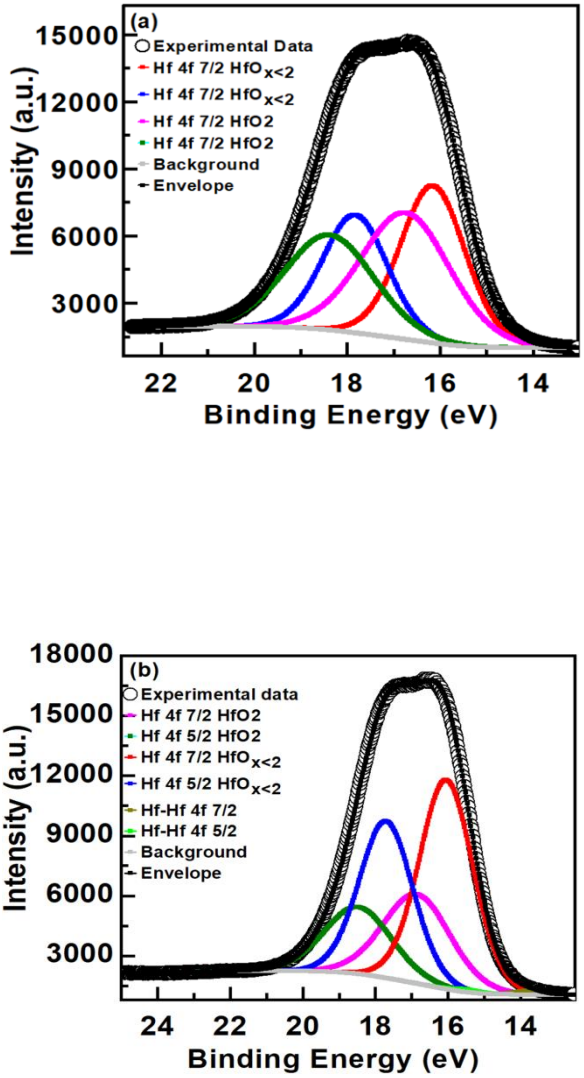
(a)
Experimental Data
Hf 4f 7/2 HfO x<2
Hf 4f 7/2 HfO x<2
Hf 4f 7/2 HfO2
Hf 4f 7/2 HfO2
Background
Envelope
Intensity (a.u.)
15000
12000
9000
6000
3000
22
20
18
16
14
Binding Energy (eV)
(b)
Experimental data
Hf 4f 7/2 HfO2
Hf 4f 5/2 HfO2
Hf 4f 7/2 HfO x<2
Hf 4f 5/2 HfO x<2
Hf-Hf 4f 7/2
Hf-Hf 4f 5/2
Background
Envelope
Intensity (a.u.)
18000
15000
12000
9000
6000
3000
24
22
20
18
16
14
Binding Energy (eV)

Fig. 3

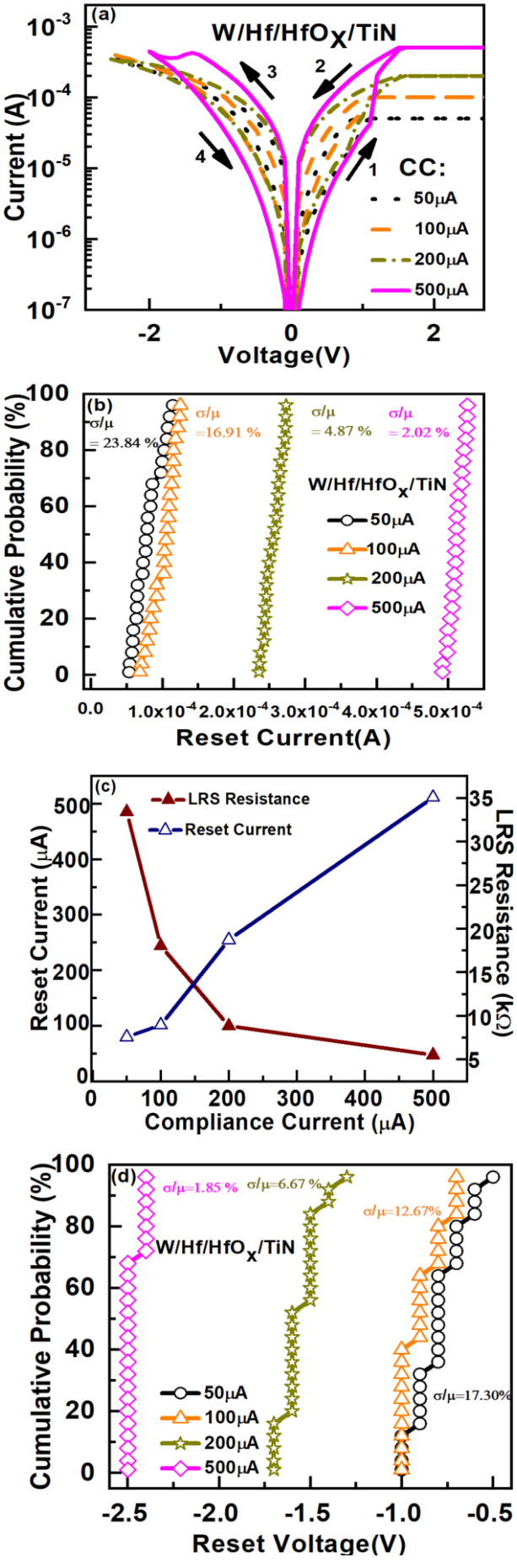
(a)
W/Hf/HfOX/TiN
Current (A)
Voltage(V)
CC:
50μA
100μA
200μA
500μA
(b)
σ/μ = 23.84 %
σ/μ =16.91 %
σ/μ = 4.87 %
σ/μ = 2.02 %
W/Hf/HfOx/TiN
Cumulative Probability (%)
Reset Current(A)
(c)
LRS Resistance
Reset Current
Reset Current (μA)
LRS Resistance (kΩ)
Compliance Current (μA)
(d)
σ/μ=1.85 %
σ/μ=6.67 %
σ/μ=12.67%
σ/μ=17.30%
W/Hf/HfOx/TiN
Cumulative Probability (%)
Reset Voltage(V)

Fig. 4

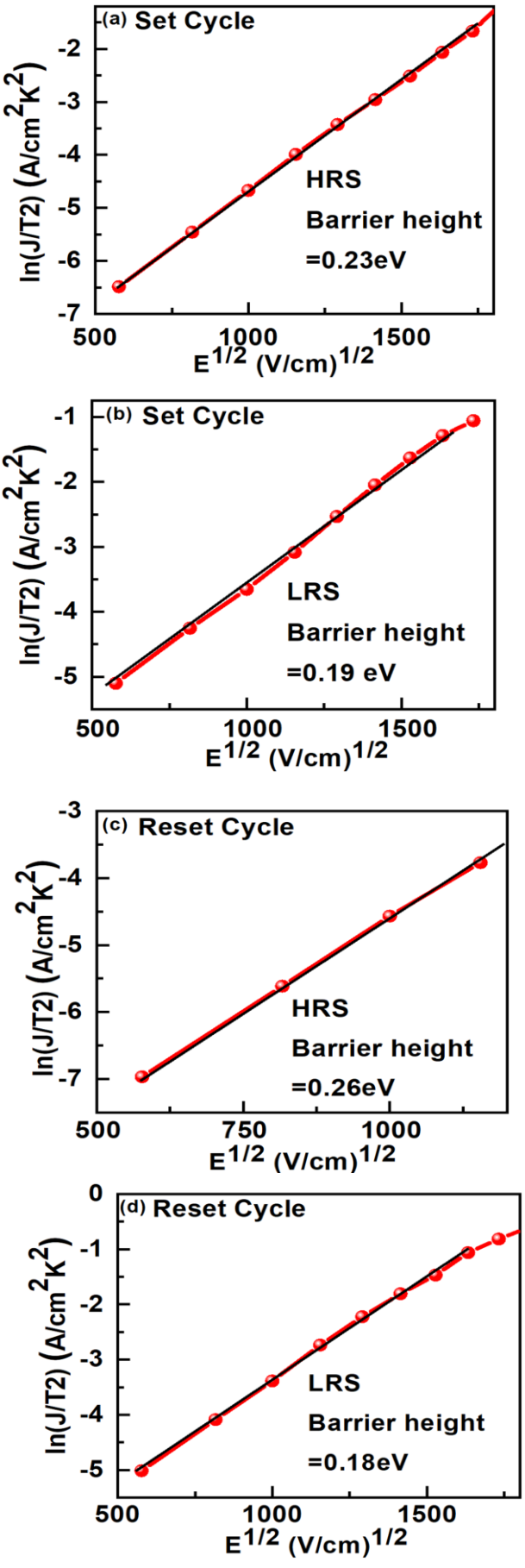
(a) Set Cycle
HRS
Barrier height
=0.23eV
ln(J/T2) (A/cm2K2)
E1/2 (V/cm)1/2
(b) Set Cycle
LRS
Barrier height
=0.19 eV
(c) Reset Cycle
HRS
Barrier height
=0.26eV
(d) Reset Cycle
LRS
Barrier height
=0.18eV

Fig. 5

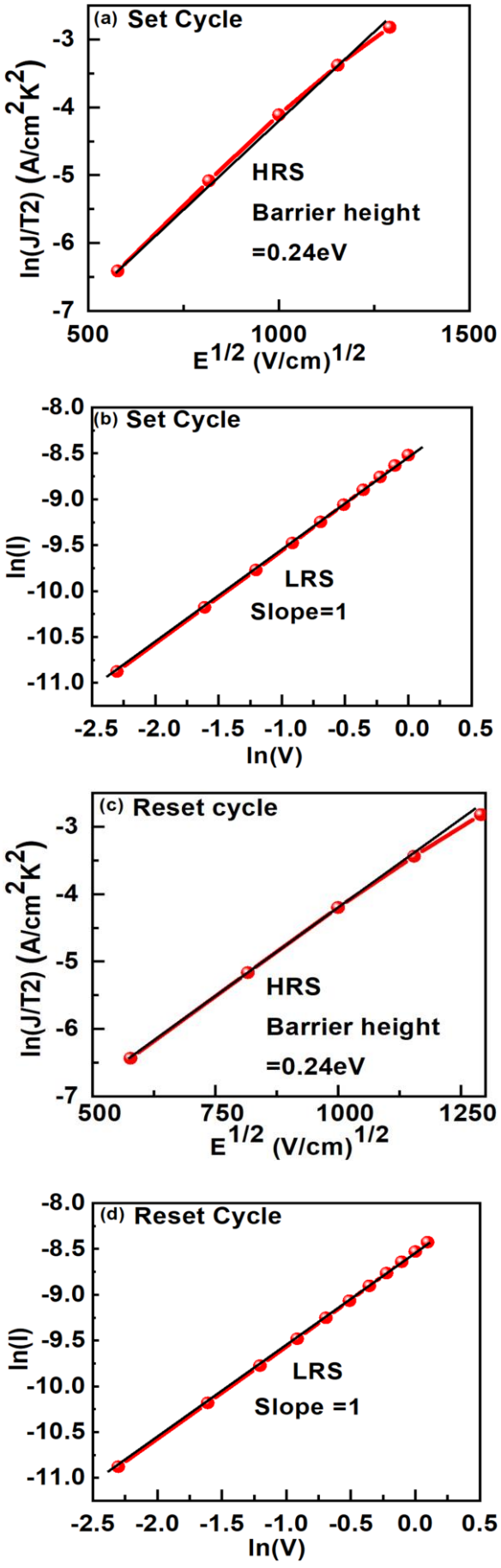
(a) Set Cycle
HRS
Barrier height
=0.24eV
ln(J/T2) (A/cm2K2)
E1/2 (V/cm)1/2
(b) Set Cycle
LRS
Slope=1
ln(I)
ln(V)
(c) Reset cycle
HRS
Barrier height
=0.24eV
ln(J/T2) (A/cm2K2)
E1/2 (V/cm)1/2
(d) Reset Cycle
LRS
Slope =1
ln(I)
ln(V)

Fig. 6

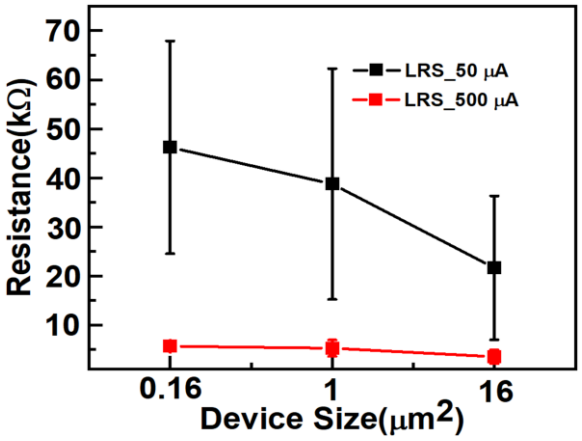
70
60
50
40
30
20
10
Resistance(kΩ)
LRS_50 μA
LRS_500 μA
0.16
1
16
Device Size(μm2)

Fig. 7

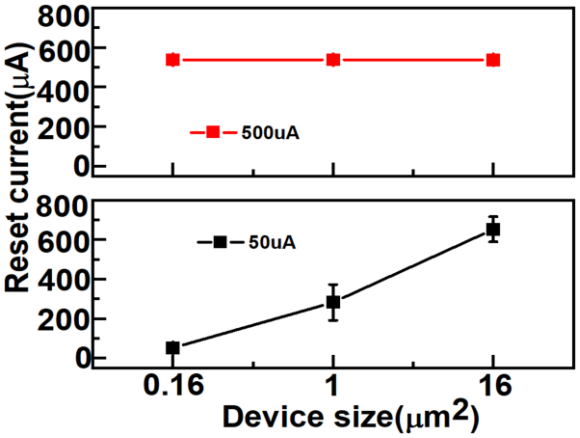
800
600
400
200
0
Reset current(μA)
500uA
800
600
400
200
0
50uA
0.16
1
16
Device size(μm2)

Fig. 8

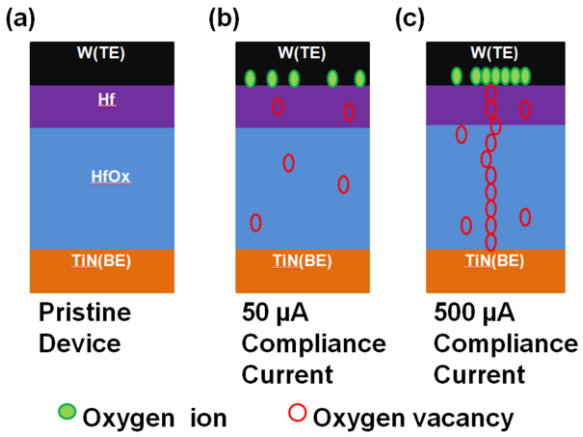
(a)
(b)
(c)
W(TE)
Hf
HfOx
TiN(BE)
Pristine Device
50 µA Compliance Current
500 µA Compliance Current
Oxygen ion
Oxygen vacancy

Fig.9

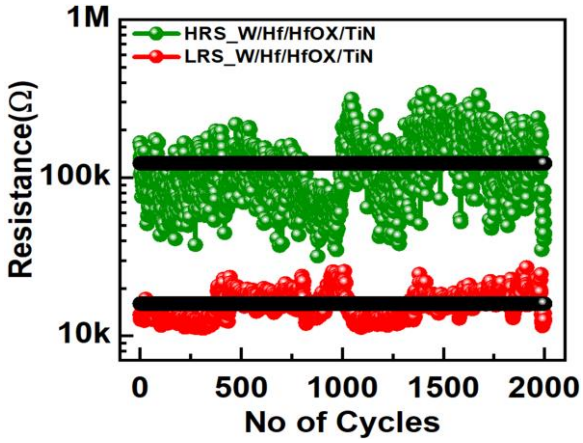
1M
100k
10k
Resistance(Ω)
HRS_W/Hf/HfOX/TiN
LRS_W/Hf/HfOX/TiN
0
500
1000
1500
2000
No of Cycles

Fig.10